

# Machine Learning for Survival Analysis: A New Approach

David Dooling<sup>1,✉</sup>, Angela Kim<sup>1,‡</sup>, Jennifer Webster<sup>1,✉</sup>

**1 Innovative Oncology Business Solutions, Albuquerque, NM, USA**

✉These authors contributed equally to this work.

‡These authors also contributed equally to this work.

\* ddooling@innovativeobs.com

## Abstract

We have applied a little-known data transformation to subsets of the Surveillance, Epidemiology, and End Results (SEER) publically available data of the National Cancer Institute (NCI) to make it suitable input to standard machine learning classifiers. This transformation properly treats the right-censored data in the SEER data and the resulting Random Forest and Multi-Layer Perceptron models predict full survival curves. Treating the 6, 12, and 60 months points of the resulting survival curves as 3 binary classifiers, the 18 resulting classifiers have AUC values ranging from .765 to .885. Further evidence that the models have generalized well from the training data is provided by the extremely high levels of agreement between the random forest and neural network models predictions on the 6, 12, and 60 month binary classifiers.

## Author Summary

Lorem ipsum dolor sit amet, consectetur adipiscing elit. Curabitur eget porta erat. Morbi consectetur est vel gravida pretium. Suspendisse ut dui eu ante cursus gravida non sed sem. Nullam sapien tellus, commodo id velit id, eleifend volutpat quam. Phasellus mauris velit, dapibus finibus elementum vel, pulvinar non tellus. Nunc pellentesque pretium diam, quis maximus dolor faucibus id. Nunc convallis sodales ante, ut ullamcorper est egestas vitae. Nam sit amet enim ultrices, ultrices elit pulvinar, volutpat risus.

## Introduction

Opportunities are emerging in many industries today to develop and deploy services that cater to individual needs and preferences. Music afficianados can create their own radio stations tailored to their individual tastes from Pandora<sup>1</sup>, bibliophiles can receive highly trustworthy book recommendations from goodreads.com<sup>2</sup>, and Google will provide directions between any two points, giving options such as mode of transportation and as well as warnings of delays in realtime.<sup>3</sup> These individualized services share many

<sup>1</sup>Pandora Internet Radio - Listen to Free Music You'll Love, <http://www.pandora.com/> (accessed 27 Jan 2016)

<sup>2</sup>Share Book Recommendations With Your Friends, Join Book Clubs, Answer Trivia, <https://www.goodreads.com/> (accessed 27 Jan 2016)

<sup>3</sup>Google Maps, <https://goo.gl/1D7Jwf> (accessed 27 Jan 2016)

common features. In particular, they leverage large databases of aggregated information to learn and extract information relevant to individuals. Extracting actionable information from data is changing the fabric of modern business. A class of techniques that transforms data into actionable information goes by the name of Machine Learning [1]. Machine Learning has recently become a popular method to answer questions and solve problems that are too complex to solve via traditional methods.

The primary objective of this study is to show how machine learning methods can be trained with data in cancer registries to produce personalized survival prognosis curves, but the methods presented below can be applied to any type of survival data. Traditionally, cancer survival curves have been estimated using Kaplan-Meier methods [2]. Kaplan-Meier methodology also uses large datasets to make predictions, but the resulting information is not personal; the resulting curves are summaries for a population and not necessarily relevant or particularly accurate for any given individual. This property of Kaplan-Meier methods is exacerbated when dealing with heterogeneous populations. The methods described below also take full advantage of all relevant aggregate information, but are able to provide personalized survival curves relevant to individual subjects. This objective is in keeping with the recent movement in medicine known as Predictive, Preventive and Personalized Medicine (PPPM), which aims to leverage increasing amounts of health related data to maximize quality of care and to intelligently eliminate inefficient and unnecessary use of resources [3]. This capability of providing individualized survival curve prognosis is a direct result of the recent advances in computing power and machine learning algorithms, and similar methodology is becoming commonplace in many industries. These techniques are now infiltrating the healthcare industry, in spite of some of the data aggregation challenges posed by the Health Insurance Portability and Accountability Act (HIPPA) of 1996. This study makes use of a freely available data source that circumvents the restrictions imposed by HIPPA.

The Surveillance, Epidemiology, and End Results (SEER) Program of the National Cancer Institute (NCI) has been collecting data because intuitively researchers feel confident that this data will eventually allow researchers to detect information crucial to patients and providers including the relationships between the types of data collected (demographic as well as staging information, treatment and disease characteristics) and the survival outcomes. Though these relationships evade capture by traditional methods, it is possible to surface them with two machine learning techniques known as *Random Forests* and *Neural Networks*. As will be demonstrated in section , these two methods produce very similar results when applied to the SEER dataset, and are based on almost diametrically opposed learning philosophies, which lends confidence in the validity of the results.

The Surveillance, Epidemiology, and End Results (SEER) Program of the National Cancer Institute (NCI) is the most recognized authoritative source of information on cancer incidence and survival in the United States. SEER currently collects and publishes cancer incidence and survival data from population-based cancer registries covering approximately 28 percent of the US population.

Quoting directly from the SEER website [4]:

The SEER program registries routinely collect data on patient demographics, primary tumor site, tumor morphology and stage at diagnosis, first course of treatment, and follow-up for vital status. This program is the only comprehensive source of population-based information in the United States that includes stage of cancer at the time of diagnosis and patient survival data. The mortality data reported by SEER are provided by the National Center for Health Statistics. The population data used in calculating cancer rates is obtained periodically from the Census Bureau.

Updated annually and provided as a public service in print and electronic formats, SEER data are used by thousands of researchers, clinicians, public health officials, legislators, policymakers, community groups, and the public.

One characteristic of the SEER data that is shared by many datasets in the medical field goes by the name of "censored data." Observations are labeled censored when the survival time information is incomplete. The SEER data contains the number of months each patient survived, as well as an indicator variable showing whether or not the patient is still alive at the end of the data collection period. Methods to deal effectively with this kind of "right-censored data" include Kaplan-Meier curves and Cox Proportional Hazard models [2]. The Kaplan-Meier techniques only give estimates for cohorts of patients and are not applicable for predicting the survival curve for a single patient, and the Cox Proportional Hazard models require a fairly restrictive set of assumptions to be satisfied in order to yield reliable results.

Previous work applying machine learning methods to subsets of the SEER data include creative attempts to deal with the problems presented by "right-censored data." Shin et al. [5] use semi-supervised learning techniques to predict 5 year survival, essentially imputing values for SEER records where the survival months information is censored at a value less than 5 years. Zolbanin et al. [6] investigate the effects of comorbidities; i.e., patients with two different cancer diagnoses, but their treatment of the censored data underestimates the survival probabilities. All records representing patients who survived at least 60 months as well as all those who died earlier than 60 months were considered, but patients alive prior to 60 months but censored out of the study before 60 months were not included. This treatment biases the data and the predictions, leading to overly pessimistic survival probabilities predicted by the models.

Previous work applying machine learning methods based on decision trees to survival data in general have a long history, starting with Gordon et al. [7]. A summary of more recent developments concerning *survival trees* is provided by Bou-Hamad et al. [8]. These methods focus on altering the splitting criteria used in decision tree growth to account for the censoring, and use 1958 Kaplan-Meier methods at the resulting nodes for prediction purposes. These methods do not generalize to non-tree-based machine learning algorithms, though Ishwaran et al. have extended the methodology to *random survival forests*, ensembles of *survival trees* [9].

IOBS has applied a little-known technique to transform the SEER data to make it amenable to more powerful machine learning methods. Instead of modifying existing learning algorithms in drastic ways, we focus attention on the input data. This approach allows for different machine learning algorithms to use the same data with no modification. The essential idea is to recast the problem to an appropriate discrete classification problem instead of a regression problem (predicting survival months). Treating months after diagnosis as just another discrete feature, the SEER data (or any other right-censored data) can be transformed to make predictions for the hazard function (probability of dying in the next month, given that the patient has not yet died). The full survival function can then be derived from the hazard function.

This paper is organized as follows. We introduce the subsets of the SEER data used for this study, and present survival curves computed from traditional methods based on this data for the three cancer types *lung*, *breast*, and *colon*. We then present the essential methodology of this work, the data transformation that allows censored survival data to be used as input to existing machine learning classifiers. Then we present the details of the trained models, including some subtleties arising from the data transformation pertaining to the partition into training and test datasets. The method of deriving binary classifiers from the models' predictions for the survival curves is presented. In this paper, we have constructed binary classifiers corresponding to 6, 12, and 60 months, as these are standard metrics in cancer survival prognosis. Then follows

a discussion of the evaluation of the trained models. The performance metrics are the 18 AUC curves associated with the 6, 12, and 60 month survival binary classifiers for the two models associated with each cancer type. We also present additional evidence supporting validity of the predictions by computing the levels of agreement between the random forest and neural network models for each of the 18 binary classifiers and find striking agreement. Next we provide urls for 6 web applications that use the trained models to predict individual cancer survival prognosis curves. These apps are hosted on the popular Heroku website, and allow for exploration of the nonlinear relationships between the input features and resulting survival prognosis. It is exactly these kinds of tools that are the goal of Predictive, Preventive and Personalized Medicine. Finally, we present avenues for future research.

## Materials and Methods

For this study we use the publically available 1973-2012 SEER incidence data files corresponding to colon, breast and lung cancer contained in the list below. SEER requires that researchers submit a request for the data, which includes an agreement form. Detailed documentation explaining the contents of both the incidence data files used in this study as well as a data dictionary for the 1973-2012 SEER incidence data files are available without the need to register or submit a data request [10].

- incidence\yr1973\_2012.seer9\COLRECT.txt
- incidence\yr1973\_2012.seer9\BREAST.txt
- incidence\yr1973\_2012.seer9\RESPIR.txt
- incidence\yr1992\_2012.sj\_la\_rg\_ak\COLRECT.txt
- incidence\yr1992\_2012.sj\_la\_rg\_ak\BREAST.txt
- incidence\yr1992\_2012.sj\_la\_rg\_ak\RESPIR.txt
- incidence\yr2000\_2012.ca\_ky\_lo\_nj\_ga\COLRECT.txt
- incidence\yr2000\_2012.ca\_ky\_lo\_nj\_ga\BREAST.txt
- incidence\yr2000\_2012.ca\_ky\_lo\_nj\_ga\RESPIR.txt
- incidence\yr2005\_lo\_2nd\_half\COLRECT.txt
- incidence\yr2005\_lo\_2nd\_half\BREAST.txt
- incidence\yr2005\_lo\_2nd\_half\RESPIR.txt

## Data preparation and preprocessing

A great deal of data munging is necessary before using these SEER incidence files as input into machine learning algorithms. A preprocessing step common to each of the three cancer types studied involves the SEER **STATE-COUNTY RECODE** variable. The **STATE-COUNTY RECODE** field is a state-county combination where the first two characters represent the state FIPS code and the last three digits represent the FIPS county code. The FIPS code is a five-digit Federal Information Processing Standard (FIPS) code which uniquely identifies counties and county equivalents in the United States, certain U.S. possessions, and certain freely associated states. This particular field illustrates an important characteristic of machine learning, that is, the difference between *categorical features* and *numeric features*. All input into a machine learning algorithm must be numeric, but real numbers carry with them the usually extremely useful property known as the well-ordering property. Machine learning algorithms use the well-ordering property of the real numbers to learn. But if one is tasked with encoding a categorical feature into suitable numeric format for machine learning, it is necessary to do so in a way that removes the well-ordering property [11].

As a simple example of how to correctly treat categorical variables in a machine learning context, consider the SEER variable **SEX**. This variable is encoded in the

Code	Description
1	Male
2	Female

**Table 1.** Encoding of gender in the SEER incidence files. These types of categorical variables need to be transformed via one-hot-encoding.

SEER raw data files with a numeric 1 for males and a numeric 2 for females as shown in Table (1). Values such as "Male" and "Female" encoded as numbers are dangerous because if not handled properly, they can generate bogus results [12]. Leaving the information for **SEX** as in Table (1) implies that Female is somehow greater than Male. This implied ordering affects the machine learning algorithms' convergence on a model. Simply encoding Male by 2 and Female by 1 would result in a completely different model, because of the now completely reversed ordering implied in the **SEX** variable. The proper way to transform the SEER **SEX** variable is to create two additional variables: **sex\_Male** and **sex\_Female**, and then to eliminate the variables **SEX** and **sex\_Male** (keeping both of the variables **sex\_Male** and **sex\_Female** is a redundant representation). For example,

$$\begin{array}{|c|} \hline \text{Sex} \\ \hline 1 \\ \hline \end{array} \rightarrow \begin{array}{|c|c|} \hline \text{sex\_Male} & \text{sex\_Female} \\ \hline 1 & 0 \\ \hline \end{array} \rightarrow \begin{array}{|c|} \hline \text{sex\_Female} \\ \hline 0 \\ \hline \end{array} \quad (1)$$

and

$$\begin{array}{|c|} \hline \text{Sex} \\ \hline 2 \\ \hline \end{array} \rightarrow \begin{array}{|c|c|} \hline \text{sex\_Male} & \text{sex\_Female} \\ \hline 0 & 1 \\ \hline \end{array} \rightarrow \begin{array}{|c|} \hline \text{sex\_Female} \\ \hline 1 \\ \hline \end{array} \quad (2)$$

The procedure outlined in Equations (1, 2) is known as one-hot encoding and needs to be applied to all of the nominal categorical variables in the SEER data that we wish to include in our predictive models. In particular, in order to include the geographical information contained in the SEER categorical variable **STATE-COUNTY RECODE**, it becomes necessary to create a new feature variable for each of the distinct (state,county) pairs in the data. In the United States, there are approximately 3,000 counties. Clearly, transforming the **STATE-COUNTY RECODE** data representation into distinct (state,county) columns will explode the dataset to become wider than is optimal for machine learning. Adding extra columns to your dataset, making it wider, requires more data rows (making it taller) in order for machine learning algorithms to effectively learn [11]. Because one-hot coding **STATE-COUNTY RECODE** would cause such drastic shape changes in our data, we wish to avoid doing so. Fortunately, this variable, though given as a categorical variable, is actually a recode for three ordinal variables. There is an ordering among the (state,county) columns, namely longitude, latitude, and elevation. We can transform the data in **STATE-COUNTY RECODE** into three new numerical columns: **lat**, **lng**, and **elevation**.

For example, Table (2) shows how five entries of **STATE-COUNTY RECODE** corresponding to counties within New Mexico can be represented by the **elevation**, **lat**, and **lng** features.

It is a simple exercise to construct the full lookup table from the SEER **STATE-COUNTY RECODE** variable to the corresponding three values **elevation**, **lat**, and **lng**. We use the publically available datafile from the United States Census Bureau [13] to map the state FIPS and county FIPS codes to query strings like those in the **address** field in Table (2). It is then possible to programmatically query the

**Table 2.** Example of the transformation of STATE-COUNTY RECODE to elevation, lat, and lng.

STATE-COUNTY RECODE	address	elevation	lat	lng
35001	Bernalillo+county+NM	5207.579772	35.017785	-106.629130
35003	Catron+county+NM	8089.242628	34.151517	-108.427605
35005	Chaves+county+NM	3559.931671	33.475739	-104.472330
35006	Cibola+county+NM	6443.415570	35.094756	-107.858387
35007	Colfax+county+NM	6147.749089	36.579976	-104.472330

Google Maps Geocoding API for the latitude and longitude [14], and the Google Maps Elevation API for the corresponding elevation [15]. An added benefit of this shift from the single categorical variable STATE-COUNTY RECODE to the three continuous numerical variables lat, lng, and elevation is that input into the web applications described later are not restricted to the states and counties covered in the SEER registries; in fact, the input to the models can be any address you would enter into Google Maps and calls to the Google Maps Geocoding API and the Google Maps Elevation API provide the conversion from the address string to the input variables lat, lng, and elevation. The full lookup table analogous to Table (2) is available from a GitHub repository containing supplemental information for this study [16].

This study focused on three different cancer types, namely colorectal cancer, lung cancer, and breast cancer. In the SEER data, there are instances of subjects with multiple rows; whenever a subject, or patient, is diagnosed with a new tumor, an additional record is added. In this study, we restrict attention to the data corresponding to the first record of each subject; i.e., we wish to make models that predict survival prognosis based on the data available right after diagnosis. The full set of conditions defining the subsets of the SEER data used in this study follows below.

The four COLRECT.txt files were imported into a pandas DataFrame object. This data was then filtered according to the conditions in Table (3). The RESPIR.txt and BREAST.txt files were imported into separate dataframes in similar fashion and filtered according to the conditions in Table (4) and Table (5), respectively. The SEER variable CS TUMOR SIZE records the tumor size in millimeters if known. But if not known, CS TUMOR SIZE is given as '999', to indicate that the tumor size is "Unknown; size not stated; not stated in pateint record." In this study, we discard those records, as indicated in Tables (5, 3, 4).

**Table 3.** Filters applied to the Colon Cancer data.

Column	Filter
SEQUENCE NUMBER-CENTRAL	≠ "Unspecified"
AGE AT DIAGNOSIS	≠ "Unknown age"
BIRTHDATE-YEAR	≠ "Unknown year of birth"
YEAR OF DIAGNOSIS	≥ 2004
SURVIVAL MONTHS FLAG	= "1"
CS TUMOR SIZE EXT/EVAL	≠ ""
CS TUMOR SIZE	≠ 999
SEER RECORD NUMBER	= 1
PRIMARY SITE	= "LARGE INTESTINE, (EXCL. APPENDIX)"
SEQUENCE NUMBER-CENTRAL	= 0

**Table 4.** Filters applied to the Lung Cancer data.

Column	Filter
SEQUENCE NUMBER-CENTRAL	≠ "Unspecified"
AGE AT DIAGNOSIS	≠ "Unknown age"
BIRTHDATE-YEAR	≠ "Unknown year of birth"
YEAR OF DIAGNOSIS	≥ 2004
SURVIVAL MONTHS FLAG	= "1"
CS TUMOR SIZE EXT/EVAL	≠ ""
CS TUMOR SIZE	≠ 999
SEER RECORD NUMBER	= 1
PRIMARY SITE	= "LUNG & BRONCHUS"
SEQUENCE NUMBER-CENTRAL	= 0

**Table 5.** Filters applied to the Breast Cancer data.

Column	Filter
SEQUENCE NUMBER-CENTRAL	≠ "Unspecified"
AGE AT DIAGNOSIS	≠ "Unknown age"
BIRTHDATE-YEAR	≠ "Unknown year of birth"
YEAR OF DIAGNOSIS	≥ 2004
SURVIVAL MONTHS FLAG	= "1"
CS TUMOR SIZE EXT/EVAL	≠ " "
CS TUMOR SIZE	≠ 999
SEER RECORD NUMBER	= 1
SEQUENCE NUMBER-CENTRAL	= 0

The following categorical features were one-hot encoded for each of the three datasets:

221
222

- SEX ,
  - MARITAL STATUS AT DX ,
  - RACE/ETHNICITY ,
  - SPANISH/HISPANIC ORIGIN ,
  - GRADE ,
  - PRIMARY SITE ,
  - LATERALITY ,
  - SEER HISTORIC STAGE A ,
  - HISTOLOGY RECODE--BROAD GROUPINGS ,
  - MONTH OF DIAGNOSIS ,
  - VITAL STATUS RECODE ,
- 223
224
225
226
227
228
229
230
231
232
233

and the STATE-COUNTY RECODE variable was dropped and replaced with the elevation , lat , and lng variables for all three datasets as illustrated in Table (2).

234
235

Before applying machine learning models trained with these datasets, we review below the salient features of survival analysis and censored data. We then describe in detail a method that takes full advantage of all the data, including the right-censored

236
237
238



data, and which involves a simple and intuitive transformation, culminating in the full set of features and target variable listed in the back of this report.

## Traditional Survival Analysis

Survival analysis pertains to data containing survival times, which are *intervals* between certain kinds of events, e.g.; cancer diagnosis date and expiry date. These intervals are often affected by a kind of "partial missingness" called *censoring*. Censored data must be analyzed in a special way to avoid biased estimates and bogus conclusions. Special methods have been developed long ago to analyze censored data properly.

With survival data, including the SEER data considered in this study, you may not know the exact time of death for some subjects. Some of the SEER subjects are still alive at the the time of the latest SEER data release. When the **VITAL STATUS RECODE** variable indicates that the subject is still alive, the **SURVIVAL MONTHS** variable is only a lower bound on the true number of survival months; this is called the *date of last contact* mode of censoring. You know that each subject either died on a certain date or was definitely alive up to some last-seen date (and you don't know how far beyond that date he or she may ultimately have lived). The latter situation is called a *censored* observation.

Statisticians have developed some traditional techniques to utilize the partial information contained in censored observations: the life-table method and the Kaplan-Meier method. Both of these methods make use of the partial information to provide unbiased estimates of the two fundamental concepts: - *hazard* and *survival*, both of which are functions of time:

- **The hazard rate**  $\lambda(t)$  is the probability of dying in the next small interval of time, assuming that the subject is alive right now.
- **The survival rate**  $S(t)$  is the probability of living for a certain amount of time after some starting point.

Incorrect treatment of survival data still seen in practice, and leading to biased results, includes simply excluding all subjects with a censored survival time from any survival analysis, and *imputing* (replacing) the censored (last-seen) date with some reasonable value. Both of these techniques destroy the partial information contained in the censored observations and nullify the validity of the resulting estimates for the hazard rate and survival rate [2].

In 1958, Edward L. Kaplan and Paul Meier collaborated to publish the seminal paper on how to estimate the hazard and survival rates for data containing censored observations [17]. The method is straightforward and for small datasets can be performed by hand. As an example, consider the survival data shown in Table (6). In the Kaplan-Meier calculation of the survival curve, the first step is to sort the subjects in Table (6) labeled 0 through 9 by *Survival Time* in ascending order. This process results in the first two columns (*Censored Status*, and *Survival Times*) in Table (7). The *At Risk* column decreases by one for each row; in every row a subject has either been censored out of the study or has died. The hazard rate is then computed for each value of *Survival Time* (necessarily a discrete function because the number of subjects is countable), by dividing the value in *Censored Status* by the value in *At Risk*. The hazard function is shown in the *Hazard Function* column in Table (7). It is then straightforward to calculate the survival function; 1 - hazard function represents the probability of not dying in the next interval of time, assuming that the subject has survived up until now and is represented by column *Prob of Surv*. The cumulative survival probability can then be obtained by successively multiplying all these individual time-slice probabilities together. In order to survive 2.4 years, first the subject has to



survive .5 years, then survive .75 years, 2.3 years and 2.4 years. The probability of surviving 2.4 years is then the product of these 3 probabilities and is given as .666 in Table(7) in the *Survival Function* column. The Kaplan-Meier survival estimate corresponding to the data given in Table (6) is shown in Table (7).

**Table 6.** Example data to illustate traditional Survival Analysis.

Survival Time (Years)	Censored Status
0	0.75
1	6.10
2	7.00
3	2.40
4	0.50
5	4.50
6	3.50
7	5.80
8	2.30
9	5.20

**Table 7.** Kaplan-Meier table corresponding to the example data in Table (6).

Censored Status	Survival Time	At Risk	Hazard Function	Prob of Surv	Survival Function
4	0	0.50	10	0.000000	1.000000
0	1	0.75	9	0.111111	0.888889
8	1	2.30	8	0.125000	0.875000
3	1	2.40	7	0.142857	0.857143
6	0	3.50	6	0.000000	1.000000
5	1	4.50	5	0.200000	0.800000
9	1	5.20	4	0.250000	0.750000
7	0	5.80	3	0.000000	1.000000
1	1	6.10	2	0.500000	0.500000
2	0	7.00	1	0.000000	1.000000

After the above one-hot encoding procedure, the new variable `vital.status_recode_Dead` indicates that the patient is deceased if this variable = 1, or else that the patient's record is right-censored if this variable = 0. `SURVIVAL MONTHS` and `vital.status_recode_Dead` are all that is needed to construct the Kaplan-Meier estimates for the SEER datasets. The Kaplan-Meier estimates of the survival curves for colon (Figure (1)), lung (Figure (3)), and breast cancer (Figure (2)) are constructed from the full population of cancer patients in the respective datasets. An unsatisfactory feature of these curves is that these estimates are based on populations and data with enough heterogeneity to make them not very meaningful to an indiviual. Patients with very disparate characteristics are given the same prognosis by these Kaplan-Meier survival curve estimates. Therefore it is desirable to find robust predictors for survival curves of individual subjects where the input is an individual record as opposed to a population. We present below the data transformation that allows for machine learning to be applied to censored data.

## Transformation of Censored Data for Machine Learning

In this section we describe an intuitive way to transform right-censored data appropriately so that it may be used as input to machine learning algorithms that learn

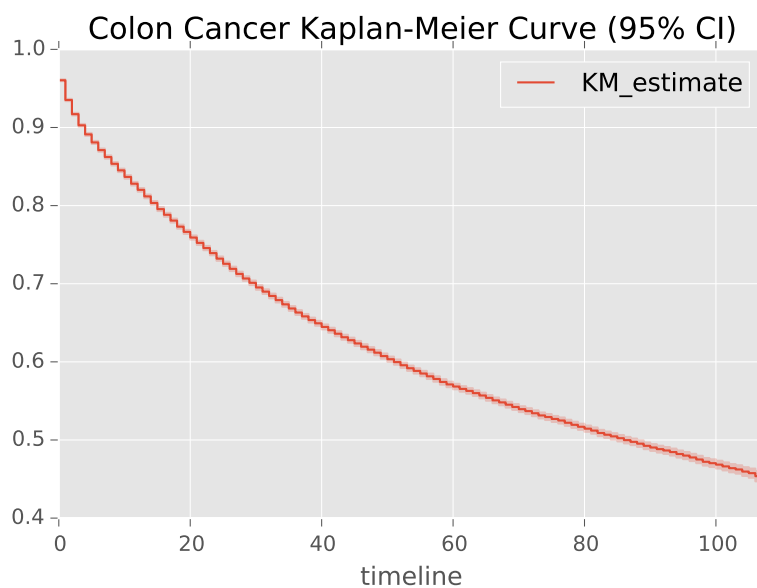


**Figure 1.** Traditional Kaplan-Meier estimate of the survival curve for all colon cancer patients. Fitted with 113072 observations, 71804 censored.

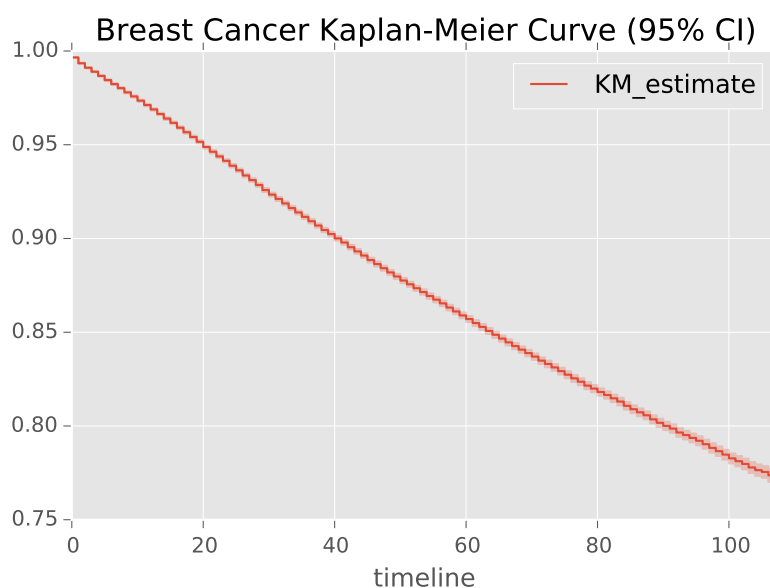


**Figure 2.** Traditional Kaplan-Meier estimate of the survival curve for all breast cancer patients. Fitted with 329949 observations, 292279 censored.

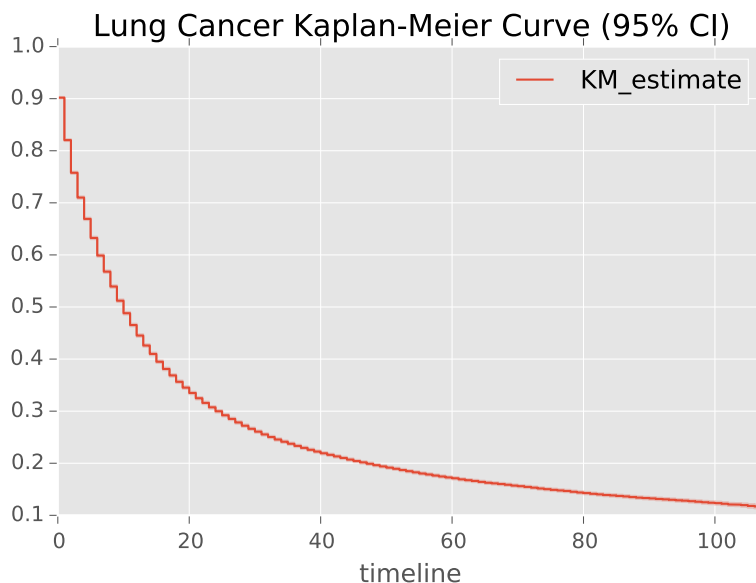


**Figure 3.** Traditional Kaplan-Meier estimate of the survival curve for all lung cancer patients. Fitted with 177089 observatins, 47409 censored.

the hazard fuction. The full details of this transformation, and a large inspiration for this study, can be flound in this blog post [18].

The overall philosophy of the Kaplan-Meier estimate of the survival curve for a population differs fundamentally from the methods described below and used in this study. The Kaplan-Meier estimate of the survival curve is given by

$$\hat{S}(t) = \prod_{t_i < t} \frac{n_i - d_i}{n_i} \quad (3)$$

where  $d_i$  are the number of death events at time  $t$  and  $n_t$  is the number of subjects at risk of death just prior to time  $t$ . Equation (3) uses the entire data set to arrive at an estimate of the entire population survival curve. In contrast, the method described below uses the entire data set to learn a model so as to predict hazard and survival curves from the data for as yet unseen individuals.

The key observation is to note that the hazard function can be directly learned via standard machine learning methods. It can be rewritten as

$$\lambda(\mathbf{X}, t) = P(Y = t | Y \geq t, \mathbf{X}), \quad (4)$$

the probability that, if someone has survived up until month  $t$ , they will die in that month. where  $\mathbf{X}$  represents all of the data for that particular record, and in our case  $Y$  represents the true, uncensored number of survival months of the patient. What is actually provided in the SEER data is the related variable **SURVIVAL MONTHS**  $T$  (how long each subject was in the study), and whether they exited by dying or being censored ( $D$ ), **VITAL STATUS RECODE** .  $D$  is a Boolean variable, so  $D = 1$  if  $T = Y$ , and  $D = 0$  if  $T < Y$ .

It follows directly from equation 4 that

$$P(Y = t | \mathbf{X}) = \lambda(\mathbf{X}, t) \prod_{i=1}^{t-1} (1 - \lambda(\mathbf{X}, i)) \quad (5)$$

, which is the full probability distribution of dying at time  $Y$  [18]. The survival function is then readily derived from this distribution as

$$S(\mathbf{X}, t) = 1 - CDF(\mathbf{X}, t) \quad (6)$$

where  $CDF(\mathbf{X}, t)$  is the cumulative density function corresponding to the probability mass function in equation 5 [12].

Treating  $T$  as just another covariate is the key to the transformation. Each datapoint in the hidden classification problem is the combination of an  $\mathbf{X}_i$  in the original dataset plus some month  $t$ , and the classification problem is "did point  $\mathbf{X}_i$  die in month  $t$ ." We will call this new variable  $D_{it}$  (**newtarget**). We can transform our original data set into a new one, with one row for each month that each  $\mathbf{X}_i$  is in the sample; train a standard classifier on this new dataset with  $D_{it}$  as the target, and derive a survival model from the original dataset. Pseudocode for this transformation is found in section Pseudocode for the Data Transformation.

Explicit examples will help make this transformation clear. The untransformed datapoint represented Table (8) is transformed to the multiple records shown in Table (10). All uncensored data is transformed in this way. All censored data is similarly transformed. The untransformed datapoint represented Table (9) is transformed to the multiple records shown in Table (11).

**Table 8.** Example of four columns in an uncensored record in the untransformed dataset.

	cs_tumor_size	year_of_birth	survival_months	vital_status_recode_Dead
newindex				
205	60	1951	3	1

**Table 9.** Example of four columns in a censored record in the untransformed dataset.

	cs_tumor_size	year_of_birth	survival_months	vital_status_recode_Dead
newindex				
205	40	1950	3	0

**Table 10.** Example of four columns in an uncensored record in the transformed dataset.

	cs_tumor_size	year_of_birth	month	newtarget
newindex				
205	60	1951	0	0
205	60	1951	1	0
205	60	1951	2	0
205	60	1951	3	1

One obvious side effect of this transformation is that it explodes the length of the dataset. For this study, the original, untransformed colon cancer DataFrame has shape (113072, 103), and the total transformed colon cancer DataFrame has shape (4165251, 103). Similarly, the original, untransformed lung cancer DataFrame has shape (177089, 115), and the total transformed lung cancer DataFrame has shape (3079931, 115). The biggest explosion in dataset size occurred with the breast cancer data, which is a consequence of the relatively high survival rates in breast cancer. A subject who is censored with a recorded survival months of 48 will contribute an extra

**Table 11.** Example of four columns in a censored record in the transformed dataset.

	cs_tumor_size	year_of_birth	month	newtarget
newindex				
205	40	1950	0	0
205	40	1950	1	0
205	40	1950	2	0
205	40	1950	3	0

48 rows to the transformed dataset. The original, untransformed breast cancer DataFrame has shape (329949, 67), and the total transformed breast cancer DataFrame has shape (15085711, 67). Training machine learning algorithms on such large datasets, even after splitting into training and testing sets described below, require large RAM. All computations for this study were performed on a Dell XPS 8700 Desktop with 32GB of RAM.

### Training and Test Partitions

After performing the data transformation adumbrated above, it is necessary to be mindful of how we partition the data into training and testing data. Each subject that was represented by a single row in the original untransformed dataset now potentially is represented by multiple rows in the transformed dataset, and care must be taken to ensure that all of the rows corresponding to a particular subject are either assigned exclusively to the training set or exclusive to the testing set. An additional characteristic of this transformed data that requires careful treatment involves balancing. The transformation results in many new records with the target variable `newtarget == 0`. The training and test sets must be chosen such that the ratio of the number of records with `newtarget == 0` to that of the number of records with `newtarget == 1` is the same in the training and test datasets. This ratio turns out to be  $\approx 396$  for the breast cancer data,  $\approx 99$  for the colon cancer data, and  $\approx 22.75$  for the lung cancer data. The shapes of the training and testing datasets for breast cancer used in this study are (14936862, 67) and (148849, 67), respectively. For lung cancer, the corresponding datasets have shapes (2988768, 115) and (91163, 115). Finally, for colon cancer the partition into training and test datasets of the transformed data have the shapes (3958008, 103) and (207243, 103). Multiple rows correspond to the same test patient in these datasets. The colon cancer test dataset represents 5654 distinct subjects; the breast cancer test dataset represents 3300 distinct subjects; and the lung test dataset contains data for 5313 distinct subjects.

The models described below are trained to learn the values of `newtarget`, which is a binary variable: a value of '0' indicating that the subject is still alive at the given month, while a value of '1' indicates that the patient died at that particular value of `months`. The random forests and neural networks described below are binary classifiers with the target `newtarget`. Fortunately, both the random forests and neural networks are capable of not only performing strict class prediction, i.e. predicting whether `newtarget` is '0' or '1', but are also able to predict the *probability* of `newtarget` being '0' or '1', and thus learning the hazard function.

Finally, we emphasize the crucial point that the features `survival_months` and `vital_status_recode_Dead` are dropped from both the training and testing data, and are replaced with the features `months` and `newtarget`, as illustrated in Tables (8, 9, 10, 11). The information of which subjects represent censored data

( `vital_status_recode_Dead == 0` ) and which died is retained and recoverable through the `newindex` variable and is needed for proper evaluation of the performance metrics; when evaluating AUC curves for the 6, 12, and 60 month binary classifiers, we need to limit the test data to those subjects that we know definitively whether or not they survived 6, 12 or 60 months respectively. This requirement will necessitate the elimination of some of the censored data when computing some of the performance metrics. We introduce the two machine learning algorithms used in this study below, chosen because of their high performance in machine learning competitions and their complementary methods, so that their mutual agreement shown below on the test datasets can be taken as indication that they are actually learning useful information.

Random Forests are made up of an ensemble of independent **Decision trees** that are purposefully exposed to only subsets of the data. The general philosophy is presented in the popular science book "The Wisdom of Crowds" [20]. The idea is that a large number of independent non-expert opinions converge on the correct answer when averaged. The success of this philosophy of prediction was startlingly shown by the success of the political and world event predictions made by the prediction market site Intrade, before its forced closure by the Commodity Futures Trading Commission [21]. The other class of methods used by IOBS to develop predictive models are called neural networks, and are modelled on how the human brain learns high level concepts from lower level ones. As opposed to the crowd-based wisdom of a random forest, a neural network is analogous to a seasoned expert. A Neural network learns from repeated exposure to the training data and improves its predictions with each pass over the data. The general philosophy is similar to that represented by the well-known maxim that it takes 10,000 hours to become an expert in any given field [22].

## Prediction Models

With the datasets transformed as described above, we are now able to use them to train and evaluate machine learning classifiers. The classifier models described in this section are learning the hazard function: given all of the data given in the Supporting Information section for each cancer type and includes the field `months` (the months after diagnosis), the models predict the target variable `newtarget`, which is a binary class label equal to 1 if the subject died in that month and 0 otherwise. Fortunately, both random forests and neural networks are capable of not only performing strict class prediction, i.e. predicting whether `newtarget` is 0 or 1, but are also able to predict the *probability* of `newtarget` being 0 or 1, and thus learning the hazard function. The models learn  $\lambda(\mathbf{X}, \text{months})$ . This prediction task should not be confused with the regression problem of trying to predict precisely in what month a patient will die.

The hazard functions thus learned and predicted are intermediary products; what we are really pursuing are the survival functions for each patient that are derived from the predicted hazard functions. From the resulting hazard functions for each unique patient, we can construct the resulting survival functions as presented in section ( ) and Equation (??) and explicitly given in python code in the notebooks at the github repository containing supplemental material for this study [16]. For each subject  $i$ , all input data minus `months` and `newtarget` is represented by  $\mathbf{X}_i$ . After the classifier models have trained with target `newtarget` on the (very large) training set, each subject's survival function is computed in the corresponding (much smaller) test set. These functions are computed by using the model to predict  $\lambda(\mathbf{X}_i, t_j)$  for  $j$  running from 0 to 120 months, and  $\mathbf{X}_i$  corresponds to the single row corresponding to subject  $i$  in the original untransformed dataset.

**Decision Trees and Random Forests** *Decision tree* classifiers are attractive models because they can be interpreted easily. Like the name decision tree suggests, we can think of this model as breaking down our data by making decisions based on asking a series of questions. Based on the features in our training set, the decision tree model learns a series of questions to infer the class labels of the samples.

*Random forests* have gained huge popularity in applications of machine learning during the last decade due to their good classification performance, scalability, and ease of use. Intuitively, a random forest can be considered as an *ensemble of decision trees*. The idea behind ensemble learning is to combine *weak learners* to build a more robust model, a *strong learner*, that has a better generalization error and is less susceptible to overfitting.

The goal behind *ensemble methods* is to combine different classifiers into a meta-classifier that has a better generalization performance than each individual classifier alone. For example, assuming that we collected predictions from 10 experts, ensemble methods would allow us to strategically combine these predictions by the 10 experts to come up with a prediction that is more accurate and robust than the predictions by each individual expert. The individual decision trees that make an ensemble are called base learners, and as long as the error rate of each base learner is less than .50, the combined random forest will benefit from the affects of combining predictions to achieve a far greater accuracy.

Figure (4) illustrates the power of ensemble methods; the Figure illustrates how the ensemble error rate is much lower than the Base learner error rate, as long as the Base learner error rate is less than 0.5. The Figure illustrates this effect for an ensemble of 500 base learners.

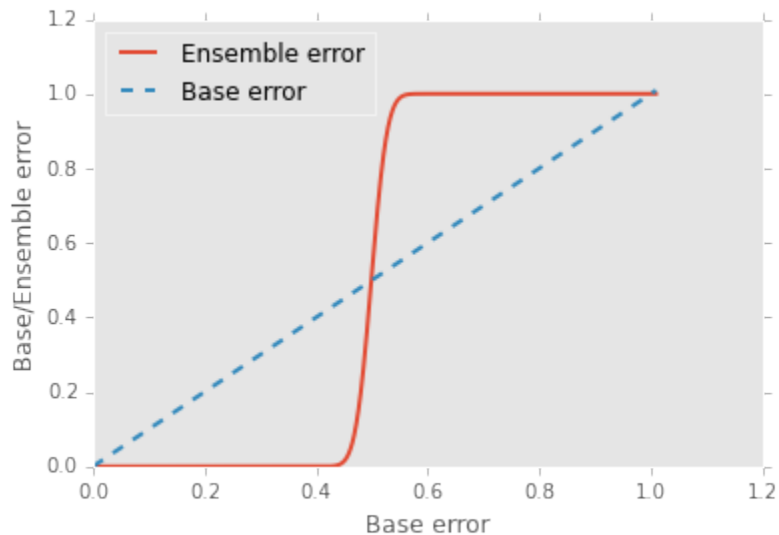


**Figure 4.** Illustration of ensemble methods showing how a collection of base learners with poor accuracy can combine to produce an accurate ensemble learner.

A big advantage of random forests is that honing in on suitable hyperparameter values (the number of trees in the forest, the depth of each decision tree, the specific measure of information gain used to choose the node splitting, etc) is not very difficult. The ensemble method is robust to noise from the individual decision trees, which helps to prevent overfitting (memorizing the training dataset targets instead of generalizing from learned rules to perform successfully on unseen data). The only parameter that has a clearly noticeable effect on performance is the number of trees to include in the forest;



in general, the more trees the better the performance, but there is a price to pay in terms of computational cost. The number of trees for the forests trained in this study was relatively small, 20 trees for breast cancer and 25 for both the lung and colon cancer models.

IOBS has chosen to use the Python scikit-learn implemenation of the Random Forest machine learning classifier [23]. Random Forests are frequent winners of the Kaggle machine learning competitions [24]. The model parameters for each cancer type are given in the Supporting Information section.

472473474475476477478479

### Etiam eget sapien nibh.

480

Nulla mi mi, Fig. 5 venenatis sed ipsum varius, volutpat euismod diam. Proin rutrum vel massa non gravida. Quisque tempor sem et dignissim rutrum. Lorem ipsum dolor sit amet, consectetur adipiscing elit. Morbi at justo vitae nulla elementum commodo eu id massa. In vitae diam ac augue semper tincidunt eu ut eros. Fusce fringilla erat porttitor lectus cursus, S1 Video vel sagittis arcu lobortis. Aliquam in enim semper, aliquam massa id, cursus neque. Praesent faucibus semper libero.

481482483484485486

**Figure 5. Figure Title first bold sentence Nulla mi mi, venenatis sed ipsum varius, volutpat euismod diam.** Figure Caption Proin rutrum vel massa non gravida. Quisque tempor sem et dignissim rutrum. A: Lorem ipsum dolor sit amet. B: Consectetur adipiscing elit.

1. react
  2. diffuse free particles
  3. increment time by dt and go to 1
- 487488489

## Results

490

Nulla mi mi, venenatis sed ipsum varius, Table 12 volutpat euismod diam. Proin rutrum vel massa non gravida. Quisque tempor sem et dignissim rutrum. Lorem ipsum dolor sit amet, consectetur adipiscing elit. Morbi at justo vitae nulla elementum commodo eu id massa. In vitae diam ac augue semper tincidunt eu ut eros. Fusce fringilla erat porttitor lectus cursus, vel sagittis arcu lobortis. Aliquam in enim semper, aliquam massa id, cursus neque. Praesent faucibus semper libero.

491492493494495496

**Table 12. Table caption Nulla mi mi, venenatis sed ipsum varius, volutpat euismod diam.**

Heading1				Heading2			
cell1row1	cell2 row 1	cell3 row 1	cell4 row 1	cell5 row 1	cell6 row 1	cell7 row 1	cell8 row 1
cell1row2	cell2 row 2	cell3 row 2	cell4 row 2	cell5 row 2	cell6 row 2	cell7 row 2	cell8 row 2
cell1row3	cell2 row 3	cell3 row 3	cell4 row 3	cell5 row 3	cell6 row 3	cell7 row 3	cell8 row 3

Table notes Phasellus venenatis, tortor nec vestibulum mattis, massa tortor interdum felis, nec pellentesque metus tortor nec nisl. Ut ornare mauris tellus, vel dapibus arcu suscipit sed.

### LOREM and IPSUM Nunc blandit a tortor.

497

Maecenas convallis mauris sit amet sem ultrices gravida. Etiam eget sapien nibh. Sed ac ipsum eget enim egestas ullamcorper nec euismod ligula. Curabitur fringilla pulvinar

498499

lectus consectetur pellentesque. Quisque augue sem, tincidunt sit amet feugiat eget, ullamcorper sed velit. Sed non aliquet felis. Lorem ipsum dolor sit amet, consectetur adipiscing elit. Mauris commodo justo ac dui pretium imperdiet. Sed suscipit iaculis mi at feugiat.

## Sed ac quam id nisi malesuada congue.

Nulla mi mi, venenatis sed ipsum varius, volutpat euismod diam. Proin rutrum vel massa non gravida. Quisque tempor sem et dignissim rutrum. Lorem ipsum dolor sit amet, consectetur adipiscing elit. Morbi at justo vitae nulla elementum commodo eu id massa. In vitae diam ac augue semper tincidunt eu ut eros. Fusce fringilla erat porttitor lectus cursus, vel sagittis arcu lobortis. Aliquam in enim semper, aliquam massa id, cursus neque. Praesent faucibus semper libero.

### Subsection 1

Nulla mi mi, venenatis sed ipsum varius, volutpat euismod diam. Proin rutrum vel massa non gravida. Quisque tempor sem et dignissim rutrum. Lorem ipsum dolor sit amet, consectetur adipiscing elit. Morbi at justo vitae nulla elementum commodo eu id massa. In vitae diam ac augue semper tincidunt eu ut eros. Fusce fringilla erat porttitor lectus cursus, vel sagittis arcu lobortis. Aliquam in enim semper, aliquam massa id, cursus neque. Praesent faucibus semper libero.

### Subsection 2

**3rd Level Heading.** Nulla mi mi, venenatis sed ipsum varius, volutpat euismod diam. Proin rutrum vel massa non gravida. Quisque tempor sem et dignissim rutrum. Lorem ipsum dolor sit amet, consectetur adipiscing elit. Morbi at justo vitae nulla elementum commodo eu id massa. In vitae diam ac augue semper tincidunt eu ut eros. Fusce fringilla erat porttitor lectus cursus, vel sagittis arcu lobortis. Aliquam in enim semper, aliquam massa id, cursus neque. Praesent faucibus semper libero.

## Discussion

Nulla mi mi, venenatis sed ipsum varius, Table 12 volutpat euismod diam. Proin rutrum vel massa non gravida. Quisque tempor sem et dignissim rutrum. Lorem ipsum dolor sit amet, consectetur adipiscing elit. Morbi at justo vitae nulla elementum commodo eu id massa. In vitae diam ac augue semper tincidunt eu ut eros. Fusce fringilla erat porttitor lectus cursus, vel sagittis arcu lobortis. Aliquam in enim semper, aliquam massa id, cursus neque. Praesent faucibus semper libero.

## LOREM and IPSUM Nunc blandit a tortor.

CO<sub>2</sub> Maecenas convallis mauris sit amet sem ultrices gravida. Etiam eget sapien nibh. Sed ac ipsum eget enim egestas ullamcorper nec euismod ligula. Curabitur fringilla pulvinar lectus consectetur pellentesque. Quisque augue sem, tincidunt sit amet feugiat eget, ullamcorper sed velit.

Sed non aliquet felis. Lorem ipsum dolor sit amet, consectetur adipiscing elit. Mauris commodo justo ac dui pretium imperdiet. Sed suscipit iaculis mi at feugiat. Ut neque ipsum, luctus id lacus ut, laoreet scelerisque urna. Phasellus venenatis, tortor nec vestibulum mattis, massa tortor interdum felis, nec pellentesque metus tortor nec nisl. Ut ornare mauris tellus, vel dapibus arcu suscipit sed. Nam condimentum sem eget

mollis euismod. Nullam dui urna, gravida venenatis dui et, tincidunt sodales ex. Nunc  
est dui, sodales sed mauris nec, auctor sagittis leo. Aliquam tincidunt, ex in facilisis  
elementum, libero lectus luctus est, non vulputate nisl augue at dolor. For more  
information, see S1 Text.

## Supporting Information

### Colon Cancer Feature Selection

The feature set used as input into both the Random Forest and Neural Network models,  
after the transformation described in section Transformation of Censored Data for  
Machine Learning is given below and also available in full detail in the file  
`NewPatientColonML.html`.

- `cs_tumor_size`
- `elevation`
- `grade_cell` type not determined
- `grade_moderately` differentiated
- `grade_poorly` differentiated
- `grade_undifferentiated`; anaplastic
- `grade_well` differentiated
- `histology_recode_broad_groupings_acinar` cell neoplasms
- `histology_recode_broad_groupings_adenomas` and adenocarcinomas
- `histology_recode_broad_groupings_blood_vessel` tumors
- `histology_recode_broad_groupings_complex` epithelial neoplasms
- `histology_recode_broad_groupings_complex_mixed` and stromal neoplasms
- `histology_recode_broad_groupings_cystic`, mucinous and serous neoplasms
- `histology_recode_broad_groupings_ductal` and lobular neoplasms
- `histology_recode_broad_groupings_epithelial` neoplasms, NOS
- `histology_recode_broad_groupings_fibromatous` neoplasms
- `histology_recode_broad_groupings_germ_cell` neoplasms
- `histology_recode_broad_groupings_lipomatous` neoplasms
- `histology_recode_broad_groupings_miscellaneous` bone tumors
- `histology_recode_broad_groupings_myomatous` neoplasms
- `histology_recode_broad_groupings_neuroepitheliomatous` neoplasms
- `histology_recode_broad_groupings_nevi` and melanomas
- `histology_recode_broad_groupings_paragangliomas` and glomus tumors
- `histology_recode_broad_groupings_soft_tissue` tumors and sarcomas, NOS
- `histology_recode_broad_groupings_squamous_cell` neoplasms
- `histology_recode_broad_groupings_synovial-like` neoplasms
- `histology_recode_broad_groupings_transistional` cell papillomas and carcinomas
- `histology_recode_broad_groupings_unspecified` neoplasms
- `lat`
- `laterality_Left`: origin of primary
- `laterality_Not` a paired site
- `laterality_Only` one side involved, right or left origin unspecified
- `laterality_Paired` site, but no information concerning laterality; midline tumor
- `laterality_Right`: origin of primary
- `lng`
- `marital_status_at_dx_Divorced`
- `marital_status_at_dx_Married` (including common law)
- `marital_status_at_dx_Separated`
- `marital_status_at_dx_Single` (never married)

• marital_status_at_dx_Unknown	591
• marital_status_at_dx_Unmarried or domestic partner	592
• marital_status_at_dx_Widowed	593
• month_of_diagnosis_Apr	594
• month_of_diagnosis_Aug	595
• month_of_diagnosis_Dec	596
• month_of_diagnosis_Feb	597
• month_of_diagnosis_Jan	598
• month_of_diagnosis_Jul	599
• month_of_diagnosis_Jun	600
• month_of_diagnosis_Mar	601
• month_of_diagnosis_May	602
• month_of_diagnosis_Nov	603
• month_of_diagnosis_Oct	604
• month_of_diagnosis_Sep	605
• number_of primaries	606
• race_ethnicity_Amerian Indian, Aleutian, Alaskan Native or Eskimo	607
• race_ethnicity_Asian Indian	608
• race_ethnicity_Asian Indian or Pakistani	609
• race_ethnicity_Black	610
• race_ethnicity_Chinese	611
• race_ethnicity_Fiji Islander	612
• race_ethnicity_Filipino	613
• race_ethnicity_Guamanian	614
• race_ethnicity_Hawaiian	615
• race_ethnicity_Hmong	616
• race_ethnicity_Japanese	617
• race_ethnicity_Kampuchean	618
• race_ethnicity_Korean	619
• race_ethnicity_Laotian	620
• race_ethnicity_Melanesian	621
• race_ethnicity_Micronesian	622
• race_ethnicity_New Guinean	623
• race_ethnicity_Other	624
• race_ethnicity_Other Asian	625
• race_ethnicity_Pacific Islander	626
• race_ethnicity_Pakistani	627
• race_ethnicity_Polynesian	628
• race_ethnicity_Samoan	629
• race_ethnicity_Thai	630
• race_ethnicity_Tongan	631
• race_ethnicity_Unknown	632
• race_ethnicity_Vietnamese	633
• race_ethnicity_White	634
• seer_historic_stage_a_Distant	635
• seer_historic_stage_a_In situ	636
• seer_historic_stage_a_Localized	637
• seer_historic_stage_a_Regional	638
• seer_historic_stage_a_Unstaged	639
• sex_Female	640
• spanish_hispanic_origin_Cuban	641
• spanish_hispanic_origin_Dominican Republic	642

- spanish\_hispanic\_origin\_Mexican
- spanish\_hispanic\_origin\_Non-Spanish/Non-hispanic
- spanish\_hispanic\_origin\_Other specified Spanish/Hispanic origin (excludes Dominican Repuclic)
- spanish\_hispanic\_origin\_Puerto Rican
- spanish\_hispanic\_origin\_South or Central American (except Brazil)
- spanish\_hispanic\_origin\_Spanish surname only
- spanish\_hispanic\_origin\_Spanish, NOS; Hispanic, NOS; Latino, NOS
- spanish\_hispanic\_origin\_Uknown whether Spanish/Hispanic or not
- year\_of\_birth
- year\_of\_diagnosis
- month

and `newtarget` is the target variable, indicating whether or not the subject died in month given by the value of the `month` variable.

## Lung Cancer Feature Selection

The feature set used as input into both the Random Forest and Neural Network models, after the transformation described in section Transformation of Censored Data for Machine Learning is given below and also available in full detail in the file `NewPatientLungML.html` .

- cs\_tumor\_size
- elevation
- grade\_cell type not determined
- grade\_moderately differentiated
- grade\_poorly differentiated
- grade\_undifferentiated; anaplastic
- grade\_well differentiated
- histology\_recode\_broad\_groupings\_acinar cell neoplasms
- histology\_recode\_broad\_groupings\_adenomas and adenocarcinomas
- histology\_recode\_broad\_groupings\_blood vessel tumors
- histology\_recode\_broad\_groupings\_complex epithelial neoplasms
- histology\_recode\_broad\_groupings\_complex mixed and stromal neoplasms
- histology\_recode\_broad\_groupings\_cystic, mucinous and serous neoplasms
- histology\_recode\_broad\_groupings\_ductal and lobular neoplasms
- histology\_recode\_broad\_groupings\_epithelial neoplasms, NOS
- histology\_recode\_broad\_groupings\_fibroepithelial neoplasms
- histology\_recode\_broad\_groupings\_fibromatous neoplasms
- histology\_recode\_broad\_groupings\_germ cell neoplasms
- histology\_recode\_broad\_groupings\_gliomas
- histology\_recode\_broad\_groupings\_granular cell tumors & alveolar soft part sarcomas
- histology\_recode\_broad\_groupings\_lipomatous neplasms
- histology\_recode\_broad\_groupings\_miscellaneous bone tumors
- histology\_recode\_broad\_groupings\_miscellaneous tumors
- histology\_recode\_broad\_groupings\_mucoepidermoid neoplasms
- histology\_recode\_broad\_groupings\_myomatous neoplasms
- histology\_recode\_broad\_groupings\_myxomatous neoplasms
- histology\_recode\_broad\_groupings\_nerve sheath tumors
- histology\_recode\_broad\_groupings\_neuroepitheliomatous neoplasms
- histology\_recode\_broad\_groupings\_nevi and melanomas

• histology_recode_broad_groupings_osseous and chondromatous neoplasms	692
• histology_recode_broad_groupings_paragangliomas and glomus tumors	693
• histology_recode_broad_groupings_soft tissue tumors and sarcomas, NOS	694
• histology_recode_broad_groupings_squamous cell neoplasms	695
• histology_recode_broad_groupings_synovial-like neoplasms	696
• histology_recode_broad_groupings_thymic epithelial neoplasms	697
• histology_recode_broad_groupings_transistional cell papillomas and carcinomas	698
• histology_recode_broad_groupings_trophoblastic neoplasms	699
• histology_recode_broad_groupings_unspecified neoplasms	700
• lat	701
• laterality_Bilateral involvement, lateral origin unknown; stated to be single primary	702
• laterality_Left: origin of primary	703
• laterality_Not a paired site	704
• laterality_Only one side involved, right or left origin unspecified	705
• laterality_Paired site, but no information concerning laterality; midline tumor	706
• laterality_Right: origin of primary	707
• lng	708
• lng	709
• marital_status_at_dx_Divorced	710
• marital_status_at_dx_Married (including common law)	711
• marital_status_at_dx_Separated	712
• marital_status_at_dx_Single (never married)	713
• marital_status_at_dx_Unknown	714
• marital_status_at_dx_Unmarried or domestic partner	715
• marital_status_at_dx_Widowed	716
• month_of_diagnosis_Apr	717
• month_of_diagnosis_Aug	718
• month_of_diagnosis_Dec	719
• month_of_diagnosis_Feb	720
• month_of_diagnosis_Jan	721
• month_of_diagnosis_Jul	722
• month_of_diagnosis_Jun	723
• month_of_diagnosis_Mar	724
• month_of_diagnosis_May	725
• month_of_diagnosis_Nov	726
• month_of_diagnosis_Oct	727
• month_of_diagnosis_Sep	728
• number_of primaries	729
• race_ethnicity_Amerian Indian, Aleutian, Alaskan Native or Eskimo	730
• race_ethnicity_Asian Indian	731
• race_ethnicity_Asian Indian or Pakistani	732
• race_ethnicity_Black	733
• race_ethnicity_Chamorrán	734
• race_ethnicity_Chinese	735
• race_ethnicity_Fiji Islander	736
• race_ethnicity_Filipino	737
• race_ethnicity_Guamanian	738
• race_ethnicity_Hawaiian	739
• race_ethnicity_Hmong	740
• race_ethnicity_Japanese	741
• race_ethnicity_Kampuchean	742
• race_ethnicity_Korean	743

• race_ethnicity_Laotian	744
• race_ethnicity_Melanesian	745
• race_ethnicity_Micronesian	746
• race_ethnicity_New Guinean	747
• race_ethnicity_Other	748
• race_ethnicity_Other Asian	749
• race_ethnicity_Pacific Islander	750
• race_ethnicity_Pakistani	751
• race_ethnicity_Polynesian	752
• race_ethnicity_Samoan	753
• race_ethnicity_Thai	754
• race_ethnicity_Tongan	755
• race_ethnicity_Unknown	756
• race_ethnicity_Vietnamese	757
• race_ethnicity_White	758
• seer_historic_stage_a_Distant	759
• seer_historic_stage_a_In situ	760
• seer_historic_stage_a_Localized	761
• seer_historic_stage_a_Regional	762
• seer_historic_stage_a_Unstaged	763
• sex_Female	764
• spanish_hispanic_origin_Cuban	765
• spanish_hispanic_origin_Dominican Republic	766
• spanish_hispanic_origin_Mexican	767
• spanish_hispanic_origin_Non-Spanish/Non-hispanic	768
• spanish_hispanic_origin.Other specified Spanish/Hispanic origin (excludes Dominican Repuclic)	769
• spanish_hispanic_origin.Puerto Rican	770
• spanish_hispanic_origin.South or Central American (except Brazil)	771
• spanish_hispanic_origin.Spanish surname only	772
• spanish_hispanic_origin.Spanish, NOS; Hispanic, NOS; Latino, NOS	773
• spanish_hispanic_origin.Uknown whether Spanish/Hispanic or not	774
• year_of_birth	775
• year_of_diagnosis	776
• month	777

## Breast Cancer Feature Selection 779

The feature set used as input into both the Random Forest and Neural Network models, after the transformation described in section Transformation of Censored Data for Machine Learning is given below and also available in full detail in the file `NewPatientBreastML.html` . 780  
781  
782  
783

• cs_tumor_size	784
• elevation	785
• grade_moderately differentiated	786
• grade_poorly differentiated	787
• grade_ndifferentiated; anaplastic	788
• grade_well differentiated	789
• histology_recode_broad_groupings_adenomas and adenocarcinomas	790
• histology_recode_broad_groupings_adnexal and skin appendage neoplasms	791
• histology_recode_broad_groupings_basal cell neoplasms	792
• histology_recode_broad_groupings_complex epithelial neoplasms	793



• histology_recode_broad_groupings_cystic, mucinous and serous neoplasms	794
• histology_recode_broad_groupings_ductal and lobular neoplasms	795
• histology_recode_broad_groupings_epithelial neoplasms, NOS	796
• histology_recode_broad_groupings_nerve sheath tumors	797
• histology_recode_broad_groupings_unspecified neoplasms	798
• lat	799
• laterality_Bilateral involvement, lateral origin unknown; stated to be single primary	800
• laterality_Paired site, but no information concerning laterality; midline tumor	801
• laterality_Right: origin of primary	802
• lng	803
• lng	804
• marital_stats_at_dx_Divorced	805
• marital_stats_at_dx_Married (including common law)	806
• marital_stats_at_dx_Separated	807
• marital_stats_at_dx_Single (never married)	808
• marital_stats_at_dx_Unknown	809
• marital_stats_at_dx_Unmarried or domestic partner	810
• marital_stats_at_dx_Widowed	811
• month_of_diagnosis_Apr	812
• month_of_diagnosis_Aug	813
• month_of_diagnosis_Dec	814
• month_of_diagnosis_Feb	815
• month_of_diagnosis_Jan	816
• month_of_diagnosis_Jul	817
• month_of_diagnosis_Jun	818
• month_of_diagnosis_Mar	819
• month_of_diagnosis_May	820
• month_of_diagnosis_Nov	821
• month_of_diagnosis_Oct	822
• month_of_diagnosis_Sep	823
• race_ethnicity_Amerian Indian, Aletian, Alaskan Native or Eskimo	824
• race_ethnicity_Asian Indian	825
• race_ethnicity_Black	826
• race_ethnicity_Chinese	827
• race_ethnicity_Japanese	828
• race_ethnicity_Melanesian	829
• race_ethnicity_Other	830
• race_ethnicity_Other Asian	831
• race_ethnicity_Pacific Islander	832
• race_ethnicity_Thai	833
• race_ethnicity_Unknown	834
• race_ethnicity_Vietnamese	835
• race_ethnicity_White	836
• seer_historic_stage_a_Distant	837
• seer_historic_stage_a_In sit	838
• seer_historic_stage_a_Localized	839
• seer_historic_stage_a_Unstaged	840
• sex_Female	841
• spanish_hispanic_origin_Cuban	842
• spanish_hispanic_origin_Mexican	843
• spanish_hispanic_origin_Non-Spanish/Non-hispanic	844
• spanish_hispanic_origin.Other specified Spanish/Hispanic origin (excldes	845

- Dominican Republic)
- spanish\_hispanic\_origin.Spanish surname only
- spanish\_hispanic\_origin.Spanish, NOS; Hispanic, NOS; Latino, NOS
- year\_of\_birth
- year\_of\_diagnosis
- month

and `newtarget` is the target variable, indicating whether or not the subject died in month given by the value of the `month` variable.

and `newtarget` is the target variable, indicating whether or not the subject died in month given by the value of the `month` variable.

## Pseudocode for the Data Transformation

```
def train(X, T, D)
    // X, T, D are the original dataset
    X' = []
    D' = []

    // the transformation
    for each index i in X:
        for t=1 to T[i]:
            new_D = (0 if t < T[i], else D[i])
            append new_D to D'
            new_X = (X[i], t)
            append new_X to X'

    return a decision tree trained on (X', D')
```

```
def pmf(h, X)
    // X is a single datapoint
    // returns an array A where A[i] = P(Y = i | X)
    A = []
    p_so_far = 1 // this is p(T >= t | X)
    for t = 1 to (the last month where h has any data):
        // h knows p(T = t | T >= t, X), we call this p_cur
        p_cur = h's prediction for (X, t)
        append (p_so_far * p_cur) to A
        p_so_far *= (1 - p_cur)
```

## Breast Random Forest Model Hyperparameters

```
f = RandomForestClassifier(n_estimators=20,min_samples_split=3,
                           max_depth = 15,
                           max_features = .8,
                           n_jobs=5,verbose=2,random_state=33)
```

## Colon Random Forest Model Hyperparameters

```
rf = RandomForestClassifier(n_estimators=25,min_samples_split=3,
                           max_depth = 10,
                           max_features = .5,
```

```
n_jobs=5,verbose=2,random_state=3)
```

## Lung Random Forest Model Hyperparameters

```
rf = RandomForestClassifier(n_estimators=25,min_samples_split=3,
                           max_depth = 11,
                           max_features = .8,
                           n_jobs=5,verbose=2,random_state=3)
```

## Breast Neural Network Model Architecture

The architecture of the Keras multilayer perceptron neural network model trained on the breast cancer data is given explicitly below:

```
modelbreast = Sequential()
modelbreast.add(Dense(114, input_shape=(66,) ,init='normal'))
modelbreast.add(Activation('relu'))
modelbreast.add(Dropout(0.05))
modelbreast.add(Dense(50, init='normal'))
modelbreast.add(Activation('relu'))
modelbreast.add(Dropout(0.05))

modelbreast.add(Dense(36, init='normal'))
modelbreast.add(Activation('relu'))
modelbreast.add(Dropout(0.05))

modelbreast.add(Dense(2, init='normal'))
modelbreast.add(Activation('softmax'))

rms = RMSprop(lr=0.001)

modelbreast.compile(loss='binary_crossentropy',
                    optimizer=rms, class_mode="binary")
```

and trained with a batch size of 1500 for 200 epochs.

## Colon Cancer Neural Network Model Architecture

The architecture of the Keras multilayer perceptron neural network model trained on the colon cancer data is given explicitly below:

```
modelcolon = Sequential()
modelcolon.add(Dense(114, input_shape=(102,) ,init='normal'))
modelcolon.add(Activation('relu'))
modelcolon.add(Dropout(0.05))
modelcolon.add(Dense(50, init='normal'))
modelcolon.add(Activation('relu'))
modelcolon.add(Dropout(0.05))

modelcolon.add(Dense(35, init='normal'))
```

```

modelcolon.add(Activation('relu'))
modelcolon.add(Dropout(0.05))

modelcolon.add(Dense(2, init='normal'))
modelcolon.add(Activation('softmax'))

rms = RMSprop(lr=0.001)

modelcolon.compile(loss='binary_crossentropy',
                   optimizer=rms, class_mode="binary")

and trained with a batch size of 1500 for 200 epochs.

```

## Lung Cancer Neural Network Model Architecture

The architecture of the Keras multilayer perceptron neural network model trained on the lung cancer data is given explicitly below:

```

modellung = Sequential()
modellung.add(Dense(114, input_shape=(114,) ,init='normal'))
modellung.add(Activation('relu'))
modellung.add(Dropout(0.1))
modellung.add(Dense(80, init='normal'))
modellung.add(Activation('relu'))
modellung.add(Dropout(0.1))
modellung.add(Dense(40, init='normal'))
modellung.add(Activation('relu'))
modellung.add(Dropout(0.1))

modellung.add(Dense(2, init='normal'))
modellung.add(Activation('softmax'))

rms = RMSprop(lr=0.001)

modellung.compile(loss='binary_crossentropy',
                  optimizer=rms, class_mode="binary")

and trained with a batch size of 2000 for 50 epochs.

```

## S1 Video

**Bold the first sentence.** Maecenas convallis mauris sit amet sem ultrices gravida. Etiam eget sapien nibh. Sed ac ipsum eget enim egestas ullamcorper nec euismod ligula. Curabitur fringilla pulvinar lectus consectetur pellentesque.

## S1 Text

**Lorem Ipsum.** Maecenas convallis mauris sit amet sem ultrices gravida. Etiam eget sapien nibh. Sed ac ipsum eget enim egestas ullamcorper nec euismod ligula. Curabitur fringilla pulvinar lectus consectetur pellentesque.

## S1 Fig

**Lorem Ipsum.** Maecenas convallis mauris sit amet sem ultrices gravida. Etiam eget sapien nibh. Sed ac ipsum eget enim egestas ullamcorper nec euismod ligula. Curabitur fringilla pulvinar lectus consectetur pellentesque.

## S2 Fig

**Lorem Ipsum.** Maecenas convallis mauris sit amet sem ultrices gravida. Etiam eget sapien nibh. Sed ac ipsum eget enim egestas ullamcorper nec euismod ligula. Curabitur fringilla pulvinar lectus consectetur pellentesque.

## S1 Table

**Lorem Ipsum.** Maecenas convallis mauris sit amet sem ultrices gravida. Etiam eget sapien nibh. Sed ac ipsum eget enim egestas ullamcorper nec euismod ligula. Curabitur fringilla pulvinar lectus consectetur pellentesque.

## Acknowledgments

Cras egestas velit mauris, eu mollis turpis pellentesque sit amet. Interdum et malesuada fames ac ante ipsum primis in faucibus. Nam id pretium nisi. Sed ac quam id nisi malesuada congue. Sed interdum aliquet augue, at pellentesque quam rhoncus vitae.

## References

1. Sebastian Raschka. Python Machine Learning Essentials. Packt Publishing; 2015.
2. Cam Davidson-Pilon. Quickstart – lifelines 0.8.0.1 documentation; 2016 (accessed 14 Jan 2016).  
<http://lifelines.readthedocs.org/en/latest/Quickstart.html>.
3. Van Poucke S, Zhang Z, Schmitz M, Vukicevic M, Laenen MV, Celi LA, et al. Scalable predictive analysis in critically ill patients using a visual open data analysis platform. PLoS ONE. 2016;11(1). Cited By 0. Available from:  
<http://www.scopus.com/inward/record.url?eid=2-s2.0-84953931466&partnerID=40&md5=7a0cad7137c03146e4b75f3295f84cc6>.
4. National Cancer Institute, the Surveillance, Epidemiology, and End Results Program. About the SEER Program - SEER; 2016 (accessed 14 Jan 2016).  
<http://seer.cancer.gov/about>.
5. Shin, Hyunjung and Nam, Yonghyun; ISCB Asia. A coupling approach of a predictor and a descriptor for breast cancer prognosis [Article; Proceedings Paper]. BMC MEDICAL GENOMICS. 2014 MAY 8;7(1). 3rd Annual Translational Bioinformatics Conference (TBC) / ISCB-Asia, Seoul, SOUTH KOREA, OCT 02-04, 2013.
6. Zolbanin, Hamed Majidi and Delen, Dursun and Zadeh, Amir Hassan. Predicting overall survivability in comorbidity of cancers: A data mining approach [Article]. DECISION SUPPORT SYSTEMS. 2015 JUN;74:150–161.

7. Gordon L, Olshen RA. Tree-structured survival analysis. *Cancer Treatment Reports*. 1985;69(10):1065–1068. Cited By 97. Available from: <http://www.scopus.com/inward/record.url?eid=2-s2.0-0021875130&partnerID=40&md5=9e112ed840960f801b6260b23bf6811d>.
8. Bou-Hamad I, Larocque D, Ben-Ameur H. A review of survival trees. *Statistics Surveys*. 2011;5:44–71. Cited By 15. Available from: <http://www.scopus.com/inward/record.url?eid=2-s2.0-84857308440&partnerID=40&md5=f8af82017ade68e335fd258c6857bf49>.
9. Ishwaran H, Kogalur UB. Consistency of random survival forests. *Statistics and Probability Letters*. 2010;80(13-14):1056–1064. Cited By 26. Available from: <http://www.scopus.com/inward/record.url?eid=2-s2.0-77953020220&partnerID=40&md5=1e4478c51150f0159fdc6c1cb631968b>.
10. National Cancer Institute, the Surveillance, Epidemiology, and End Results Program. Documentation for ASCII Text Data Files - SEER Datasets; 2016 (accessed 15 Jan 2016). <http://seer.cancer.gov/data/documentation.html>.
11. Michael Bowles. *Machine Learning in Python: Essential Techniques for Predictive Analysis*. Wiley; 2015.
12. Allen Downey. *Think Stats*. O'Reilly Media; 2014.
13. United States Census Bureau. 2010 FIPS Code Files for Counties - Geography - U.S. Census Bureau; 2016 (accessed 18 Jan 2016). <https://www.census.gov/geo/reference/codes/cou.html>.
14. Google Developers. The Google Maps Geocoding API — Google Maps Geocoding API — Google Developers; 2016 (accessed 18 Jan 2016). <https://developers.google.com/maps/documentation/geocoding/intro>.
15. Google Developers. The Google Maps Elevation API — Google Maps Elevation API — Google Developers; 2016 (accessed 18 Jan 2016). <https://developers.google.com/maps/documentation/elevation/intro?hl=en>.
16. IOBS. Supplemental Material — PAPERDATA; 2016 (accessed 18 Jan 2016). <https://github.com/doolingdavid/PAPERDATA.git>.
17. Kaplan EL, Meier P. Nonparametric Estimation from Incomplete Observations. *Journal of the American Statistical Association*. 1958;53(282):457–481. Cited By 34216. Available from: <http://www.scopus.com/inward/record.url?eid=2-s2.0-33845382806&partnerID=40&md5=1b3d05fab93fcd0e37f176c799b3cfff6>.
18. Ben Kuhn. *Decision trees for survival analysis*; 2016 (accessed 14 Jan 2016). <http://www.benkuhn.net/survival-trees>.
19. Northeastern Illinois Chapter, American Statistical Association. *Survival Analysis: Introduction*; 2005 (accessed 27 Jan 2016). [http://www.amstat.org/chapters/northeasternillinois/pastevents/presentations/summer05\\_Ibrahim\\_J.pdf](http://www.amstat.org/chapters/northeasternillinois/pastevents/presentations/summer05_Ibrahim_J.pdf).
20. James Surowiecki. *The Wisdom of Crowds*. Doubleday; 2004.
21. John Cassidy. What killed Intrade?; 13 Mar 2013 (accessed 25 Jan 2016). <http://www.newyorker.com/news/john-cassidy/what-killed-intrade>.

22. Malcolm Gladwell. *Outliers*. Back Bay Books; 2011.
23. scikit-learn developers. 3.2.4.3.1. `sklearn.ensemble.RandomForestClassifier`; 2014 (accessed 25 Jan 2016). <http://scikit-learn.org/stable/modules/generated/sklearn.ensemble.RandomForestClassifier.html>.
24. Kaggle Inc . Random Forests — Kaggle; 2015 (accessed 25 Jan 2016). <https://www.kaggle.com/wiki/RandomForests>.